Pattern selection and control via localized feedback

Andreas Handel
Department of Biology, Emory University, Atlanta, Georgia 30322, USA

Roman O. Grigoriev
School of Physics, Georgia Institute of Technology, Atlanta, Georgia 30332-0430, USA
(Received 15 August 2005; published 14 December 2005)

Many theoretical analyses of feedback control of pattern-forming systems assume that feedback is applied at every spatial location, something that is often difficult to accomplish in experiments. This paper considers an experimentally more feasible scenario where feedback is applied at a sparse array of discrete spatial locations. We show how such feedback can be computed analytically for a class of reaction-diffusion systems and use generalized linear stability analysis to determine how dense the actuator array needs to be to select or maintain control of a given pattern state in the presence of noise. The one-dimensional Swift-Hohenberg equation is used to illustrate our theoretical results and explain earlier experimental observations on the control of the Rayleigh-Bénard convection.

DOI: 10.1103/PhysRevE.72.066208 PACS number(s): 05.45.Gg, 02.30.Yy

I. INTRODUCTION

Nonequilibrium spatially extended systems have a prominent place in physics, chemistry, biology, and engineering. Fluid flows, plasmas, and wide-aperture semiconductor lasers provide a few technologically important examples. As these systems are driven farther from equilibrium, they tend to display progressively more complicated dynamics, transitioning from spatially uniform to spatially patterned states and eventually developing spatiotemporal chaos. To make the best use of these systems, we need to learn to control them, forcing the system to choose one of the suitable states, even though such states might be naturally unstable. Flow control for drag reduction or noise suppression represents arguably the best known application [1].

Neither fluids nor plasma can be practically controlled at every point in space. Although recent advances in micro-electro-mechanical systems technology in certain instances enable real-time independent control at millions of locations with spatial resolution on the scale of tens of microns [2], more typically one is forced to control the dynamics by applying feedback at relatively few locations. A good example would be a tokamak with feedback applied by varying the current in a discrete and relatively small set of magnetic coils [3]. It is, therefore, important to understand the limitations of localized control of spatially extended dynamics and the physical mechanisms which determine the minimal number or density of actuators that is needed for successful stabilization of a given system.

Serving as a motivation for this study is another example of the localized control of a pattern forming system provided by the experiments of Tang and Bau [4], who attempted to maintain the laterally uniform no-motion state of the fluid in the Rayleigh-Bénard convection above the primary instability threshold using an array of sensors (thermal diodes) and actuators (resistive heaters). The heat flux generated by each of the 24 heaters embedded in the bottom boundary was taken to be a linear function of the temperature deviation (relative to the conductive profile) measured by the diode located at the midplane of a cylindrical convection cell directly above the heater. The authors noted that the degree of stabilization obtained in the experiments fell far short of their own theoretical prediction [5] that the critical Rayleigh number for the onset of convection in a laterally infinite fluid layer can be postponed by as much as an order of magnitude. The discrete nature of the sensor and actuator arrays was quoted as a possible reason: the theoretical work assumed that the actuators and sensors were continuously distributed in space, while in the experiment it was necessary to use a finite number of sensors and actuators.

In the absence of environmental noise, the minimal number of actuators and sensors needed to control the fluid inside a convection cell is, in fact, uniquely determined by the dimensionality of the largest irreducible representation of the symmetry group of the linearized system [6]. For a cylindrical convection cell the symmetry group is O(2), so just a pair of sensors and a pair of actuators is sufficient to stabilize a noiseless system (although a more elaborate feedback is needed than that used in the experiments by Tang and Bau). In the presence of noise a much larger number of sensors and actuators might be necessary. The goal of the present theoretical study is to determine how this number depends on the strength of the noise, the size of the system, and the specifics of the dynamics. Although the equations describing the Rayleigh-Bénard convection are well known, they do not allow us to perform all computations in purely analytic form, so instead we will use a one-dimensional Swift-Hohenberg equation [7] which describes the emergence of a straight roll convective pattern just above the onset of the primary instability. Focusing on scalar one-dimensional equations will also allow us to generalize the results for a much wider class of reaction-diffusion systems.

The paper is organized as follows. In Sec. II we describe our model system and summarize previous research relevant to this study. Section III presents the computation of the feedback gain and its scaling analysis. In Sec. IV we characterize the transient growth of disturbances in the system, and use these results to determine the number of actuators re-

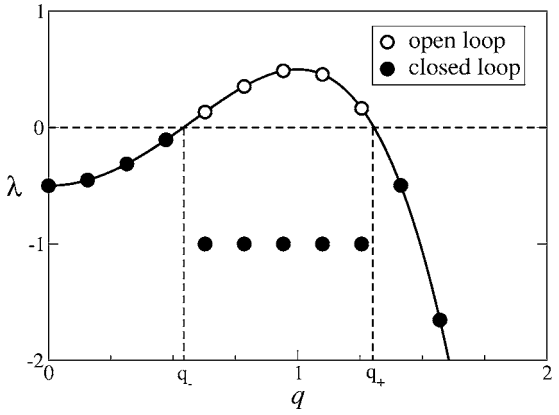

FIG. 1. The eigenvalue spectrum of the Swift-Hohenberg equation with $\epsilon=0.5$. The solid line represents the spectrum of a laterally infinite open loop system. The circles represent the spectrum of the system on a finite domain of length $l=40$.

quired for successful control. We then proceed to discuss control of patterned states in Sec. VI and present our conclusions in Sec. VII. The appendices contain the algebra omitted from the main text to streamline the exposition.

II. THE MODEL

Although the following analysis applies to a broad class of pattern-forming systems, for illustration purposes it will be convenient for us to concentrate on a particular example of the Swift-Hohenberg equation:

$$\partial_t \phi = \epsilon\phi - (1+\partial_x^2)^2\phi - \phi^3, \tag{1}$$

where $\phi(x,t)$ could describe temperature and velocity disturbances relative to the laterally uniform no-motion state and ϵ is the reduced control parameter describing how strongly the system is driven out of equilibrium by the imposed heat flux. The eigenvalues of the linearization about the uniform state $\phi_0(x,t)\equiv 0$ are

$$\lambda(q) = \epsilon - (1-q^2)^2 \tag{2}$$

with the largest one $\lambda(1)=\epsilon$, so that ϵ also measures the distance to the onset of primary instability for the laterally infinite system.

Once ϵ becomes positive, the uniform state becomes unstable and a periodic pattern emerges with a period corresponding to some wave numbers in the unstable band $q_- < q < q_+$, where $q_\pm = \sqrt{1\pm\sqrt{\epsilon}}$ (see Fig. 1). This pattern can be easily found in the form of an asymptotic Fourier series

$$\phi_q(x,t) = \sum_n a_n \cos(nqx), \tag{3}$$

which quickly converges for moderate ϵ. All even coefficients vanish, $a_2=a_4=a_6=\cdots=0$, while the odd coefficients can be found using the method of dominant balance:

$$a_1 = \frac{2}{\sqrt{3}}\epsilon^{1/2}\cos\theta + \sqrt{3}\epsilon^{3/2}\cos^3\theta\left(\frac{1}{576} + \frac{1}{256}\epsilon^{1/2}\sin\theta + \frac{61}{9216}\epsilon - \frac{2941}{442\,368}\epsilon\cos^2\theta + \cdots\right),$$

$$a_3 = -\sqrt{3}\epsilon^{3/2}\cos^3\theta\left(\frac{1}{288} + \frac{1}{128}\epsilon^{1/2}\sin\theta + \frac{61}{4608}\epsilon - \frac{163}{12288}\epsilon\cos^2\theta + \cdots\right),$$

$$a_5 = \frac{\sqrt{3}}{165888}\epsilon^{5/2}\cos^5\theta + \cdots,$$

$$\cdots, \tag{4}$$

where we have defined $\sqrt{\epsilon}\sin\theta = 1-q^2$, such that the unstable band of wave numbers q maps exactly onto the interval $-\pi<\theta<\pi$ for any ϵ. Standard analysis shows that the patterned states ϕ_q near the edges of the stable band (i.e., $\sqrt{\epsilon/3} < |1-q^2| < \sqrt{\epsilon}$ for an unbounded system), are unstable and, without feedback, undergo a secondary (Eckhaus) instability toward another pattern $\phi_{q'}$ with q' closer to the center of the unstable band.

Both the uniform state ϕ_0 and the patterned states ϕ_q could be stabilized for $\epsilon>0$ by applying feedback using a finite number of actuators whose action is assumed to be spatially localized, as is typically the case in practice. In the following we will concentrate on the limiting case where the region of the system affected by each actuator is so small that the feedback can be described by a δ function. Alternatively, control could be envisioned as a way to select a pattern, if the system size l and/or ϵ is large enough for several patterned states to coexist. Our goal here is to determine how the number of actuators depends on l and ϵ, or more generally, on the choice of the evolution equation.

Nonlinear control of infinite-dimensional dynamics such as those displayed by reaction-diffusion systems is still in its infancy, despite some attempts to apply weakly nonlinear analysis tools such as the center manifold reduction [8]. For the most part feedback control of this class of systems is based on the same foundation as the theory of pattern formation-linear stability analysis. This more popular approach, however, has a significant limitation—it describes only the asymptotic stability of the system with respect to infinitesimal disturbances. This presents a problem in describing real (e.g., finite size) disturbances which can transiently grow, before the asymptotic exponential decay sets in, to become large enough to invalidate the linear approximation on which the whole analysis is based, leading to a control breakdown. Transient, or algebraic, growth of spontaneous disturbances has attracted a lot of attention recently, mostly in the context of transition to turbulence in shear flows, leading to the development of a generalized linear stability analysis [9–11].

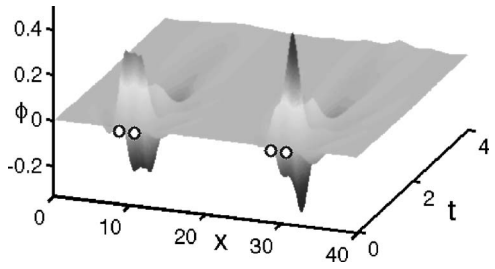

FIG. 2. Time evolution of an initial disturbance (random noise with magnitude $\sigma=10^{-4}$) for the Swift-Hohenberg equation (1) with periodic boundary conditions and $\epsilon=0.5$. Localized feedback control is applied at four points marked with circles. For a system of size $l=40$ the disturbance transiently grows by several orders of magnitude before exponential decay to the uniform target state $\phi(x,t)=0$ takes over.

We illustrate this phenomenon in Figs. 2 and 3, which show the dynamics of the Swift-Hohenberg equation with localized feedback control (to be discussed in detail in the following sections). Up to a certain system size, transient growth does not effect our ability to stabilize the system and eventually exponential decay to the uniform target state is achieved, as Fig. 2 shows. However, for larger system sizes, transient growth becomes so strong that control is no longer able to suppress the initial disturbance, as seen in Fig. 3.

In fact, such transient growth should be found in most pattern-forming systems evolving in the presence of localized feedback, as can be inferred from the following simple argument. Imagine a spontaneous disturbance localized between two actuators. Since the actuators cannot directly affect the region where the disturbance originated, the feedback has to propagate from the location of the actuators toward the disturbance. During the time it takes for the feedback to propagate towards and quench the disturbance, the latter grows in an essentially uncontrolled way. Once the feedback reaches the perturbed region of the system, the disturbance is being suppressed until it completely vanishes (or another disturbance is spontaneously created somewhere in the system).

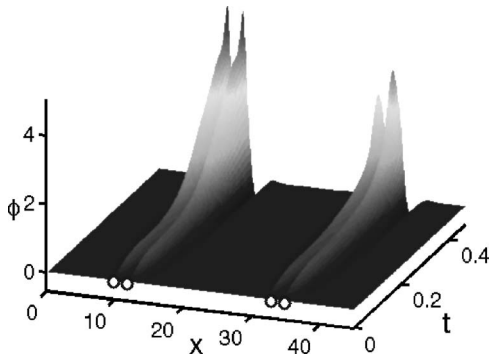

FIG. 3. The evolution of a random initial disturbance (same as in Fig. 2) in the Swift-Hohenberg equation on a larger domain, $l=45$. Here the transient growth of the disturbance is strong enough for nonlinearities to become important, leading to the failure of linear control. The system eventually diverges from the target state $\phi(x,t)=0$.

Extreme sensitivity of the controlled (closed loop) dynamics to spontaneous disturbances stemming from their transient growth has been discovered by one of us [12], while Egolf and Socolar, were the first to link transient growth to the strong non-normality of the evolution operator describing the dynamics of disturbances in a coupled map lattice (CML) [13]. We have recently extended their results to a system described by a partial differential equation (PDE) [14]. In particular, we showed that non-normality arises as a result of imposing localized feedback, even when the uncontrolled (open loop) system is normal. Furthermore, we showed that transient growth increases exponentially with the system size in both PDEs [14] and CMLs [12]. In another study [15], we showed that control failure can be described by a combined action of transient growth and nonlinearity, which triggers a nonlinear instability. The work presented here significantly extends and generalizes the ideas presented in Ref. [14].

III. FEEDBACK CONTROL OF THE UNIFORM STATE

We will start our analysis by concentrating on the localized feedback control of the uniform state $\phi_0(x,t)=0$. Feedback control of other steady states is conceptually similar, however, the high degree of symmetry of the uniform state makes it special. On the one hand, control of that state is, in some sense, the most challenging, since it requires the largest number of independent actuators in the zero noise limit. On the other hand, this higher symmetry allows a much greater degree of analytical progress.

We will start by considering how the feedback control setup needs to be modified as the system size l is increased from very small to very large (with $\epsilon>0$ held fixed). If the domain size is sufficiently small (e.g., $l<2\pi/\sqrt{1+\sqrt{\epsilon}}$ for periodic boundary conditions), the uniform state is stable due to strong confinement effects and no control is needed.

A. Control at one boundary

Systems of a somewhat larger size can be successfully controlled by placing a single actuator at one of the boundaries. Linear feedback control can be implemented by modulating the flux of a quantity characterizing the state of the system, e.g., mass, temperature, or concentration, through a boundary (here $x=l$):

$$\phi'(l,t)=\int_0^l k(x)\phi(x,t)dx, \tag{5}$$

where, as usual, the prime denotes the spatial derivative. In the case of the Rayleigh-Bénard convection, for instance, one could control the dynamics of the fluid by changing the heat flux through a boundary of the convection cell [4,16]. Then the feedback gain $k(x)$ would describe how temperature disturbances in different regions inside the cell affect the flux. There is a lot of flexibility in choosing the three remaining boundary conditions (since the Swift-Hohenberg equation is the fourth order), as long as they are consistent with the target state. Here it is convenient for us to pick them as

$$\phi(0,t) = \phi''(0,t) = \phi'''(l,t) = 0. \tag{6}$$

The spectrum of the open loop $[k(x)=0]$ system linearized about the target state is discrete, with eigenfunctions

$$f_n(x) = \sin(q_n x), \quad q_n = \frac{(2n-1)\pi}{2l}, \quad n = 1,2,\ldots \tag{7}$$

and eigenvalues given by (2). The eigenfunctions $f_n(x)$ are orthogonal—which means the linearized evolution operator for the open loop system is normal—and form a convenient basis for the stability analysis of the closed loop system.

Projecting the linearized evolution equation onto the basis (7), we obtain an infinite system of coupled ordinary differential equations (ODEs)

$$\dot{\Phi}_n = \lambda_n \Phi_n - (-1)^n \sum_{m=1}^{\infty} K_m \Phi_m \equiv (M\Phi)_n, \tag{8}$$

for the Fourier coefficients $\Phi_n(t)$ and K_n of $\phi(x,t)$ and $k(x)$, respectively,

$$\phi(x,t) = \sum_{n=1}^{\infty} \Phi_n(t) f_n(x),$$

$$k(x) = \sum_{n=1}^{\infty} K_n f_n(x). \tag{9}$$

As we show in Appendix A, the eigenvalues of the system (8) can be changed by modifying the feedback gain coefficients K_m. For instance, replacing s consecutive eigenvalues $\lambda_a \to \lambda_a', \ldots, \lambda_b \to \lambda_b'$ requires

$$K_m = \frac{(-1)^m \prod_{p=a}^{b} (\lambda_m - \lambda_p')}{\prod_{p=a}^{m-1} (\lambda_m - \lambda_p) \prod_{p=m+1}^{b} (\lambda_m - \lambda_p)} \tag{10}$$

for $m=a,\ldots,b$ and setting the rest to zero. Making all new eigenvalues negative and using (9) allows us to determine the feedback gain $k(x)$ which renders the system linearly stable with new eigenvalues $\lambda_m' < 0$ that we are free to choose however we find convenient.

In principle, this result allows one to find a stabilizing feedback for *any* system size l. However, as we illustrated earlier, control eventually fails if the system size is increased without adding additional actuators. To understand the origin of control failure, we consider the behavior of the gain coefficients K_m for large l. We first rewrite (10) in exponential form

$$|K_m| = \exp\left\{ \sum_{p=a}^{b} \ln|\lambda_m - \lambda_p'| - \sum_{p=a}^{m-1} \ln|\lambda_m - \lambda_p| - \sum_{p=m+1}^{b} \ln|\lambda_m - \lambda_p| \right\}. \tag{11}$$

In the large l limit, the eigenvalues are dense enough to approximate the sums with integrals. It is natural to choose the wave number $q = q_- + (p-a)(\pi/l)$ as the integration variable, with integrals going over the unstable band of the open loop system. To leading order in l we obtain

$$|K_m| \sim \exp\left\{ \frac{l}{\pi} \left(\int_{q_-}^{q_+} \ln \frac{|\lambda_m - \lambda'(q)|}{|\lambda_m - \lambda(q)|} dq \right) \right\}. \tag{12}$$

Note that this expression includes a pair of integrable singularities at $\lambda(q) = \lambda_m$, which are excluded in (11). The singularities contribute $O(\ln l)$ terms in the argument of the exponential, which are small compared with the $O(l)$ dominant contribution and so can be ignored.

The results (10)–(12) are rather general and apply to many different systems, not just the Swift-Hohenberg equation. This allows us to draw several important conclusions. First of all, since the terms inside the parentheses in (12) are independent of l, one immediately concludes that the Fourier coefficients K_m, and hence the gain function $k(x)$, blow up exponentially with the size l of the system. Second, since all the λ_m' are negative, the strength of feedback, is minimized by choosing all new eigenvalues very close to zero, $\lambda_m' \approx 0$, $m=a,\ldots,b$. The larger the absolute value of the new eigenvalues, the stronger the feedback is required, which is an intuitively sensible conclusion.

The scaling of $k(x)$ is determined by the largest coefficient K_m. Since

$$\frac{dK_m}{dm} = \frac{\partial K_m}{\partial \lambda} \frac{\partial \lambda}{\partial q} \frac{dq}{dm}, \tag{13}$$

the maximum in K_m with respect to m corresponds to the maximum in λ with respect to q. For the Swift-Hohenberg equation the maximum of $\lambda(q)$ is achieved at $q=1$, for which $\lambda_m = \epsilon$.

We can obtain a more explicit scaling relation if we use our freedom to choose the new eigenvalues and set

$$\lambda_a' = \cdots = \lambda_b' = \Lambda < 0. \tag{14}$$

Substituting this into (12) yields

$$k_{max} \equiv \max_x |k(x)| \sim \max_m |K_m| \sim e^{l/l_0} \tag{15}$$

with the characteristic length scale l_0 specific to a particular evolution equation. For the Swift-Hohenberg equation, l_0 is given by

$$l_0 = \pi \left\{ (q_+ - q_-)[4 + \ln(\epsilon + |\Lambda|)] + 2 \ln\left[\frac{(1+q_-)(q_+-1)(1-q_-^2)^{q_-}}{(1+q_+)(1-q_-)(q_+^2-1)^{q_+}} \right] \right\}^{-1}. \tag{16}$$

To check these analytical results, we compare (15) with the maximum of the feedback gain computed numerically using two different methods. In the first, the feedback is computed directly from (10), where all positive eigenvalues are set to $\Lambda < 0$ and the negatives ones are left unchanged. This approach is known as pole placement (PP) in control theory. The second method uses the linear quadratic regulator (LQR) control. In LQR the feedback is computed as the solution minimizing a functional quadratic in $\phi(x,t)$ and

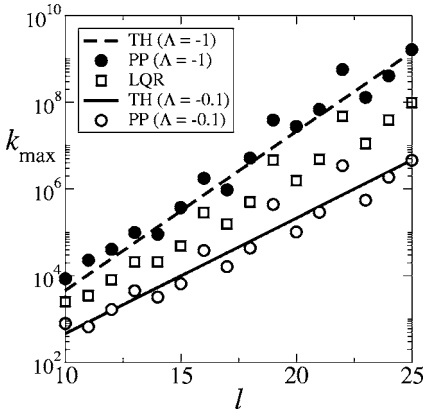

FIG. 4. Maximal feedback gain k_{max} for $\epsilon=0.75$. For LQR control, the new eigenvalues λ_k' lie between -1 and -0.1. Straight lines show the theoretical result (15). One actuator is placed on the right boundary.

$\phi'(l,t)$ [17]. In LQR, the new eigenvalues λ_k' cannot be explicitly specified. Both PP and LQR are commonly used in the control theory [18–20].

The agreement between the analytical and numerical scaling (see Fig. 4) is quite impressive despite the fact that the asymptotic results ($l\to\infty$) are used for a relatively small system size. The agreement would improve further for larger l. In particular, the fluctuations in the numerical results can be attributed to finite-size effects which would become smaller for larger l. Unfortunately, the numerical solutions become unreliable for $l\gtrapprox 25$, reflecting the fact that the Jacobian of the closed loop system becomes increasingly non-normal and hence near singular. Nevertheless, it is clear that the slope is correctly predicted by our analysis, even for system sizes that are not very large. Our numerical results also show that, according to (16), the slope increases with $|\Lambda|$, as predicted by the general scaling expression (12).

B. Control at two boundaries

By increasing the size of the system further we find that the feedback gain grows exponentially fast, eventually becoming large enough to violate the linearity assumption underlying our stability analysis. The most natural way to resolve this problem is by adding an additional actuator, placing it at the opposite boundary. With this setup the control authority is split in such a way that the left actuator is primarily responsible for suppressing disturbances in the left half of the system, while the right actuator is primarily responsible for the right half. Naively this would lead one to expect that this arrangement would be able to stabilize a system of about twice the size, all else being equal. The following analysis shows that this is indeed the case.

Let us keep the the right boundary condition incorporating the feedback term in the form (5). The action of the second actuator can be expressed in a symmetric form

$$\phi'(0,t)=\int_0^l p(x)\phi(x,t)dx \tag{17}$$

with $p(x)=-k(l-x)$. Although, in principle, one could choose the gains $p(x)$ and $k(x)$ differently by ignoring the symmetry, this would generally lead to suboptimal control [17]. The remaining boundary conditions are chosen to be $\phi'''(0,t)=\phi'''(l,t)=0$.

The eigenfunctions of the open loop system are now

$$f_n(x)=\cos(q_n x),\quad q_n=\frac{(n-1)\pi}{l},\quad n=1,2,\ldots \tag{18}$$

and eigenvalues are given by (2) as usual. Note that the eigenfunctions (18) are again orthogonal, so that the open loop evolution operator is normal.

Proceeding as before (see Appendix B for details) we find the feedback gain coefficients to be

$$K_m=\frac{(-1)^m(\lambda_m-\lambda_m')\prod_p{}'(\lambda_m-\lambda_p')}{2\prod_p{}'(\lambda_m-\lambda_p)}, \tag{19}$$

with $m=a,\ldots,b$. The prime on the products denotes that the index goes over integers $p=\ldots,(m-4),(m-2),(m+2),(m+4),\ldots$ in steps of two, with an additional restriction $a\leqslant p\leqslant b$. We further find for l large the feedback gain to scale as

$$k_{max}\sim e^{l/2l_0}, \tag{20}$$

where l_0 is still given by (16). This is exactly the same scaling relation as that found in the one-actuator case, but with a different characteristic length. The additional prefactor of $\frac{1}{2}$ in the exponent [it arises due to the fact that the product over p in (19) goes in steps of two], shows that doubling the number of actuators doubles the characteristic system size, as the naive argument made earlier would suggest.

C. Control with an array of actuators

Increasing the system size yet further we find that the two actuator setup eventually fails as well, requiring more actuators to be added. However, placing more than two actuators on the boundary is not going to improve the performance of our controller significantly, so we have to change our approach. In order to control a system of arbitrary size l using a feedback gain of a fixed magnitude, we expect to need a number of actuators r on the order of l/l_0 as the maximum distance between actuators is restricted by the characteristic length l_0. In other words, control authority is now split in such a way that each actuator is responsible for an $O(l_0)$ size segment of the system. With this more general arrangement the system is described by

$$\partial_t\phi=\epsilon\phi-(1+\partial_x^2)^2\phi-\phi^3+\sum_{p=1}^{r}d_p(x)u_p(t), \tag{21}$$

where the $d_p(x)$ are the influence functions describing the location and spatial extent of the actuators. In the limit of perfectly spatially localized control, $d_p(x)$ reduce to δ functions.

Again, to preserve the symmetry of the system, we will assume periodic boundary conditions and place the actuators in a regular array. However, we cannot arrange them periodi-

cally, as that would make the system uncontrollable [6]. We can achieve controllability (or more precisely, stabilizability) by using a periodic array of *pairs* of actuators, which corresponds to

$$d_p(x) = \begin{cases} \delta\left[x - (p-\Delta)\frac{l}{r}\right], & p\text{-odd}, \\ \delta\left[x - (p-1+\Delta)\frac{l}{r}\right], & p\text{-even}. \end{cases} \tag{22}$$

For instance, four actuators would be placed as two pairs, one pair at $x=(1\pm\Delta)l/4$ and the other at $x=(3\pm\Delta)l/4$. The spacing $2l\Delta/r$ between the two actuators in each pair has to be chosen to satisfy the stabilizability constraints [6], but is otherwise arbitrary. As a rule of thumb, stabilizability can be achieved by making the spacing smaller than the wavelength of the shortest unstable mode of the open loop system.

The functions $u_p(t)$ describe the strength of feedback and are chosen as

$$u_p(t) = \int_0^l k_p(x)\phi(x,t)dx. \tag{23}$$

Using the remaining symmetry of the problem all feedback gains $k_p(x)$ can be expressed through $k_1(x)$. Indeed, the system with the chosen arrangement of actuators remains invariant under translations by a multiple of the distance between pairs of actuators, $x \to x+nl/r$, $n=2,4,\ldots$. The feedback control preserving this symmetry requires gain functions $k_{p+2}(x)$ to have the same shape as $k_p(x)$, only shifted by $2l/r$. Further, the reflection symmetry implies that for each actuator pair the gain function for $k_{p+1}(x)$ should have the same shape as $k_p(x)$, reflected at the midpoint between the actuators. Combining these two results, we obtain

$$k_p(x) = k_1\left((-1)^p\left\{\frac{pl}{r} - \frac{l}{2r} - x\right\} + \frac{l}{2r}\right) \tag{24}$$

for $p=2,\ldots,r$. The resulting control is translationally and reflectionally symmetric, i.e., has a symmetry described by a discrete subgroup of the continuous symmetry group $O(2)$ of the open loop system. As shown in [17], such control is optimal with respect to general measures that respect the symmetry of the system.

With periodic boundary conditions, the eigenfunctions of the open loop system are Fourier modes

$$f_n(x) = e^{iq_n x}, \quad q_n = \frac{2\pi n}{l}, \quad n = -\infty, \ldots, \infty \tag{25}$$

which are orthogonal as we found previously, such that the Jacobian of the open loop system is normal. Using this basis we can again convert the PDE (21) into a system of ODEs

$$\dot{\Phi}_n = \lambda_n \Phi_n + \sum_{p=1}^{r} D_n^p \sum_{m=-\infty}^{\infty} K_{-m}^p \Phi_m, \tag{26}$$

for the Fourier coefficients of $\phi(x,t)$, $d_p(x)$ and $k_p(x)$ defined according to

$$\phi(x,t) = \sum_{n=-\infty}^{\infty} \Phi_n(t) f_n(x),$$

$$k_p(x) = \sum_{n=-\infty}^{\infty} K_n^p f_n(x),$$

$$d_p(x) = \frac{1}{l}\sum_n D_n^p f_n(x). \tag{27}$$

The calculations similar to those described previously (see Appendix C for details) give

$$K_m^1 = (K_{-m}^1)^* = C_m \frac{2(\lambda_m - \lambda_m')\prod_p{}' (\lambda_m - \lambda_p')}{r\prod_p{}' (\lambda_m - \lambda_p)}, \tag{28}$$

with $m=a,\ldots,b$. The primes on the products indicate that the index $p=\ldots,(m-r),(m-r/2),(m+r/2),(m+r),\ldots$ goes in steps of $r/2$ subject to an additional restriction $a \leqslant p \leqslant b$. The numerical prefactor is given by

$$C_m = \frac{\exp\left[\frac{2\pi i}{r} m(\Delta - 1)\right]}{\exp[2\pi i g_m \Delta] - 1}, \tag{29}$$

where g_m is a positive integer, which depends on both m and r. In the scaling analysis this prefactor is of no importance, since it is independent of both the system size l and the choice of new eigenvalues. Setting all unstable eigenvalues to $\Lambda < 0$ we obtain the feedback gain scaling in this most general case to be

$$k_{max} \sim e^{l/rl_0} \tag{30}$$

with l_0 given by (16), indicating that the characteristic length has grown by a factor of r. This result again supports our naive expectations: by employing r actuators, the system size can be increased by a factor of r without increasing the magnitude of the feedback applied by each actuator.

It is interesting to note how a particular arrangement of actuators in the array (i.e., the distance between actuators in each pair) affects the magnitude of the feedback signal. The latter depends on Δ only through the prefactors C_m, which diverge for $\Delta = n/g_m$ with any integer n, which corresponds to the loss of stabilizability. For instance, when $4m$ is an integer multiple of r, one obtains $g_m = 4m/r$, so that C_m diverges when the locations of all actuators coincide with the nodes of a Fourier mode with wave number $q = \pm 2\pi m/l$. Choosing Δ outside of small neighborhoods of such values yields $C_m = O(1)$, making the coefficients K_m^p very weakly dependent on the spacing between actuators in each pair.

IV. TRANSIENT GROWTH

As the results of numerical simulations presented in Figs. 2 and 3 illustrate, large feedback gain leads to strong tran-

sient growth of disturbances. Significant transient growth is expected in this problem due to the nonorthogonality of the eigenfunctions of the closed loop system which makes the linearization (8) non-normal. Consider, for instance the feedback at one boundary. As a result of translational invariance of our model the eigenfunctions of the linearization of (1) subject to the boundary conditions (5) and (6) all have the form $f_q(x)=\sin qx$, regardless of whether control is turned on or off. Closing the feedback loop merely shifts all wave numbers q into the stable band, at the same time destroying the mutual orthogonality of the eigenfunction set. It is easy to see that certain choices of the closed loop eigenvalues, such as (14), can force a number of closed loop eigenfunctions to align arbitrarily closely.

In this section we describe more explicitly the connection between the magnitude of feedback gain and the strength of transient growth. The latter can be described quantitatively via the transient amplification factor

$$\gamma \equiv \max_{t,\Phi(0)} \frac{\|\Phi(t)\|_2}{\|\Phi(0)\|_2} = \max_t \|e^{Mt}\|_2 = \|e^{Mt_{max}}\|_2, \tag{31}$$

which measures the maximum amplitude of an evolved disturbance $\Phi(t)$ for all possible initial conditions $\Phi(0)$. The initial condition producing the maximal amplification at time t_{max} is often called the optimal disturbance Φ_{opt} and is given by the right singular vector corresponding to the largest singular value of $e^{Mt_{max}}$ [10]. For normal operators $\gamma=1$, but for non-normal ones it can be arbitrarily large. Several authors have introduced quantities similar to (31) to characterize transient growth [10,11,21,22]. We should point out that the transient amplification factor is analogous to transfer norms, which arise in the input-output description commonly used in control theoretic analyses, including those concerning transient growth [23–25].

Since both matrix exponentials and matrix norms are difficult to compute analytically, γ as defined by (31) is usually computed numerically. Nevertheless, sometimes one can construct reasonably tight bounds without resorting to numerics, an approach that we will follow here. To that end, we first note that for small times

$$\|e^{Mt}\|_2 = 1 + \Gamma t + O(t^2), \tag{32}$$

where $\Gamma=\lambda_{max}(W)$ is the largest eigenvalue of $W=\frac{1}{2}(M+M^\dagger)$ [10]. Although this eigenvalue is also difficult to compute exactly, a lower bound can be found by using the following property of Hermitian matrices:

$$\lambda_{max}(W) = \max_{\|u\|=1} u^\dagger M u. \tag{33}$$

In the large l limit the elements of M vary by many orders of magnitude, so a tight lower bound is obtained by choosing a unit vector u which picks out the largest element of M. This largest element is $M_{nn}=\lambda_n+Q_{nn}\sim rk_{max}$ according to (C7). Therefore, choosing $u_k=\delta_{kn}$ we obtain $\lambda_{max}(W)\gtrsim rk_{max}$. Taking $t=t_{max}$ we obtain the following estimate for the maximal transient amplification:

$$\gamma \sim k_{max} t_{max}. \tag{34}$$

Since (32) is only accurate for small times, (34) should provide an accurate estimate for γ as long as t_{max} is reasonably small, i.e., when transient growth is a fast process.

In order to make further analytical progress, let us again assume that the closed loop system (21) has s identical eigenvalues $\lambda_k'=\Lambda$, $k=a,\cdots,b$. The corresponding eigenmodes are identical and therefore do not form a complete basis. Hence the Jacobian matrix M is nondiagonalizable. In this case, M can be converted into the Jordan normal form

$$J = S^{-1}MS = \begin{pmatrix} J_1 & 0 & 0 \\ 0 & J_s & 0 \\ 0 & 0 & J_2 \end{pmatrix}, \tag{35}$$

where $J_1=\mathrm{diag}(\ldots,\lambda_{a-2},\lambda_{a-1})$, J_s is an $s\times s$ Jordan block with eigenvalues $\lambda_k=\Lambda$, $J_2=\mathrm{diag}(\lambda_{b+1},\lambda_{b+2},\ldots)$, and S is the respective transformation matrix. The solution for the state $\Phi(t)$ is

$$\Phi(t) = \sum_{p<a} c_p e^{\lambda_p t} e_p + \sum_{p=a}^{b} \left[\sum_{m=0}^{b-p} c_{p+m} \frac{t^m}{m!} \right] e^{\Lambda t} \hat{e}_p + \sum_{p>b} c_p e^{\lambda_p t} e_p, \tag{36}$$

where e_p are eigenvectors corresponding to blocks J_1 and J_2, $\hat{e}_p$ are the generalized eigenvectors such that $M\hat{e}_p=\Lambda\hat{e}_p+\hat{e}_{p-1}$ for $p=a+1,\ldots,b$ and $\hat{e}_a=e_a$ is the only eigenvector of J_s. The c_p are integration constants that depend on the choice of the initial condition. The first and the last sum in (36) monotonically decay to zero (the corresponding eigenvectors are normal) and we can therefore neglect them. The second sum exhibits both the initial algebraic growth and the asymptotic exponential decay characteristic of transient dynamics. Each term in the second sum describes a mode of the closed loop system with amplitude

$$\hat{\Phi}_m(t) \sim \frac{t^m}{m!} e^{\Lambda t}, \quad m = 1, \ldots, s-1. \tag{37}$$

The maximum of $\hat{\Phi}_m$ is achieved at

$$t_m = \frac{m}{|\Lambda|}. \tag{38}$$

Substituting (38) back into (37) we obtain

$$\hat{\Phi}_m(t_m) \sim \frac{m^m e^{-m}}{m!|\Lambda|^m}. \tag{39}$$

This expression as a function of m has a single extremum inside the domain, which is a minimum. The maximum occurs either on the left or on the right boundary, that is either for $m=1$ or $m=s-1$, depending on the value of $|\Lambda|$. Using the Stirling formula we can write (39) as

$$\hat{\Phi}_m(t_m) \sim \frac{1}{\sqrt{2\pi m}|\Lambda|^m}. \tag{40}$$

This expression shows that for $|\Lambda|\gtrsim 1$, the global maximum is achieved for $m=1$, while for $|\Lambda|\lesssim 1$ the global maximum will be at $m=s-1$. In the intermediate region (for $|\Lambda|\approx 1$)

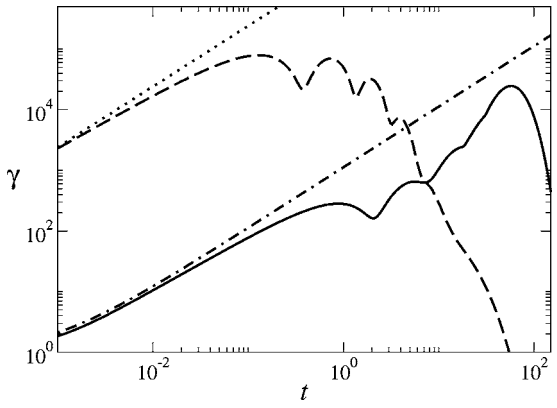

FIG. 5. Transient growth of initial disturbances for a system with $\epsilon=0.5$, two actuators, and $l=40$ ($s=8$). The solid and dashed line show the (numerically computed) exact result (31) for $\Lambda=-0.1$ and $\Lambda=-2$, respectively. The dash-dotted and dotted line show the small time approximation (32) for $\Lambda=-0.1$ and $\Lambda=-2$, respectively.

neither maximum is dominant. Approximating t_{max} with the corresponding t_m, we obtain $t_{max}|\Lambda|=s-1\sim l$ for small $|\Lambda|$ and $t_{max}|\Lambda|=1$ for large $|\Lambda|$.

Since for small $|\Lambda|$, the term with $m=s-1$ dominates, the magnitude of transiently amplified disturbances close to t_{max} should be described by

$$\hat{\Phi}_{s-1}(t) \sim \frac{t^{s-1}}{(s-1)!}e^{\Lambda t}. \tag{41}$$

In this regime t_{max} is large and we should expect (34) to produce a poor estimate of the maximum transient amplification. Indeed, Fig. 5 shows that for $\Lambda=-0.1$ the growth in $\|e^{Mt}\|_2$ is linear only for $t\ll t_{max}$ and higher order polynomial terms dominate near $t=t_{max}$.

On the other hand, for large $|\Lambda|$ the linear term with $m=1$ dominates, so the magnitude of transiently amplified disturbances is well approximated by

$$\hat{\Phi}_1(t) \sim te^{\Lambda t}. \tag{42}$$

In this regime $t_{max}\approx t_1=1/|\Lambda|$ is small and we expect (34) to produce an accurate estimate for γ. As Fig. 5 shows, one does indeed find a good agreement for $\Lambda=-2$. For large $|\Lambda|$, we can therefore combine (34) with (38) and obtain to leading order in l

$$\gamma \sim \frac{1}{|\Lambda|}e^{l/rl_0}, \tag{43}$$

where l_0 depends on both ϵ and Λ.

Just like the feedback gain, the transient amplification increases exponentially fast with the length of the system and decreases with the number of actuators. This scaling is compared with numerical results in Fig. 6. As expected, the agreement is better for $\Lambda=-2$ than for $\Lambda=-0.1$. However, even though the derivation leading to (43) breaks down for small $|\Lambda|$, we still find that γ increases exponentially fast with l.

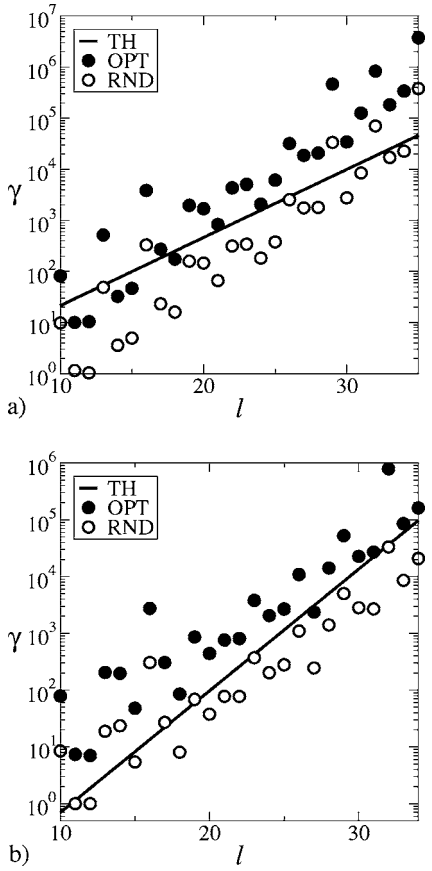

FIG. 6. Transient amplification as a function of system size l. The results are shown for two actuators placed at the boundaries with $\epsilon=0.75$ and (a) $\Lambda=-0.1$ or (b) $\Lambda=-2$. The closed and open circles show the numerical results computed for an optimal disturbance and for an ensemble of 100 random initial conditions, respectively. The straight line represents the theoretical estimate (43).

Since the optimal disturbances which produce the largest transient amplification might not be representative of typical random noise in the system, we additionally compute the amount of transient amplification $\max_t\|\Phi(t)\|_2/\|\Phi(0)\|_2$ achieved for an ensemble of random initial conditions. Figure 6 shows the maximum over a moderate number of such initial conditions. Not surprisingly, since none of the random initial conditions are optimal, they are amplified less than the optimal ones. However, transient amplification of the random initial conditions scales in the same way as γ computed from (31). This shows that (43) gives a good estimate for the transient growth of both optimal and generic random initial conditions.

This also means that the above results also generalize naturally to systems continuously driven by stochastic noise, which is the case in the majority of experimentally relevant situations. Assuming that the noise has standard deviation σ, transient growth will amplify it by a factor of order γ, such that the resulting disturbance about the target state will have a standard deviation of order $\gamma\sigma$. As a result, the noise with $\sigma=O(\gamma^{-1})$ will be amplified to $O(1)$ at which point one can effectively conclude that the control has failed. (In the next section we will see that control can fail for even weaker

noise once the effect of nonlinear terms is considered.)

The results obtained in this section still apply if we relax some of the assumptions. In the analysis presented above, we assumed that all new eigenvalues of the closed loop system are identical. This allowed us to isolate the terms in the formal solution (36) responsible for transient growth. For a more typical case when the new eigenvalues are different, the Jacobian matrix M is diagonalizable and all eigenvectors of M are distinct. Therefore, the solution (36) is not valid anymore. If, however, M is strongly non-normal with closely aligned eigenvectors, the evolution will still be characterized by strong transient growth of disturbances. In this case (32) will still hold, provided the transient growth happens on a fast enough time scale. Since t_{max} is primarily determined by the spectrum of the eigenvalues $\{\lambda_k'\}$, but is weakly dependent on the system size l, we can expect (43) to hold as well. This conclusion is supported by similar calculations we performed for other pattern forming systems (e.g., Ginzburg-Landau and Kuramoto-Sivashinsky equations), for a different number of actuators r as well as for different choices of the closed loop eigenvalues λ_k'.

V. ESTIMATION OF CONTROL FAILURE

Now that we have understood the behavior of the closed loop system in the linear approximation, we can turn our attention to the effect of nonlinear terms. Loosely speaking, once the nonlinear terms become comparable to the linear terms, the main assumption on which the linear stability analysis is based breaks down leading to failure of control. As a more careful analysis shows, at least for power law nonlinearities such as ϕ^n, the destabilization in a closed loop system can proceed along two separate routes [15]. In the first, transient dynamics (i.e., purely linear effect) amplifies an initial disturbance of magnitude σ to the point where the order of magnitude of the linear terms, $\gamma\sigma$, is comparable to that of the nonlinear terms, $(\sigma\gamma)^n$. Equating the two expressions we find a power law scaling of the critical noise level leading to destabilization

$$\sigma \propto \gamma^{\alpha}, \tag{44}$$

with exponent $\alpha=-1$.

In another route, the nonlinear terms act as a secondary disturbance, which sustains transient growth after the primary disturbance has been suppressed by feedback. In this scenario, which is sometimes referred to as bootstrapping [9,26,27], secondary disturbances can be further transiently amplified by the linear part of the evolution operator, closing a positive feedback loop, which can also lead to destabilization of the closed loop system for sufficiently large magnitudes of disturbances. The positive feedback loop produces growth in the magnitude of secondary disturbances when the order of magnitude of nonlinear terms, $(\gamma\sigma)^n$, is comparable to that of the secondary (or primary) disturbance itself, σ. Again, comparing these expressions we find a power law scaling (44), but with a different exponent $\alpha=-n/(n-1)$.

A combination (or rather a competition) of the two mechanisms is also possible, leading to a power law dependence of the critical noise level with a crossover between the two values of the exponent. This happens, for instance, for the Swift-Hohenberg equation with localized feedback (21), where the nonlinearity is cubic, $n=3$, so that one finds a crossover between $\alpha=-1$ (for smaller γ where the direct route is dominant) and $\alpha=-\frac{3}{2}$ (for larger γ where the bootstrapping route dominates). Denoting the coefficient of proportionality in (44) as C and substituting (43) we find the minimal number of actuators necessary to avoid destabilization of the closed loop system in the presence of noise to be given by

$$r \approx \frac{l}{l_0(\ln C + \ln|\Lambda| - \alpha^{-1}\ln\sigma)}. \tag{45}$$

As the numeric data shown in Figs. 7 and 8 illustrates, (45) accurately describes the dependence of the minimal number of actuators on both the system size l and the distance ϵ from the onset of primary instability, which is easily accessible experimentally, unlike the dependence on the

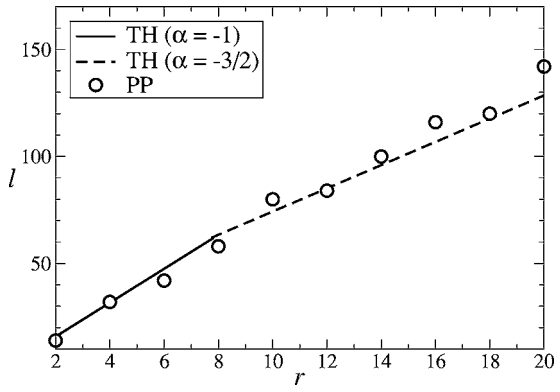

FIG. 7. Length l at which control of the uniform state fails for a given number r of actuators. We used an initial disturbance of magnitude $\sigma=10^{-3}$ and $\epsilon=0.75$. Control is calculated with new eigenvalues λ_k' spaced uniformly on the interval $(-2,-1)$. The lines represents the analytical result (45) with a crossover from $\alpha=-1$ to $\alpha=-3/2$ and $\Lambda=-1.5$.

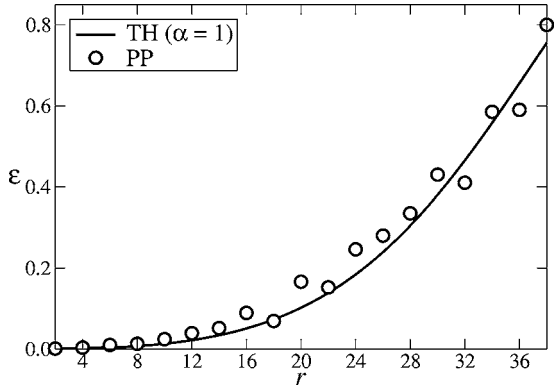

FIG. 8. Critical parameter ϵ at which control of the uniform state fails for a given number r of actuators. We used an initial disturbance of magnitude $\sigma=10^{-3}$ and $l=300$. Control is calculated with new eigenvalues λ_k' spaced uniformly on the interval $(-2,-1)$. The curve represents the analytical result (45) with $\alpha=-1$ and $\Lambda=-1.5$.

noise magnitude σ or the transient amplification factor γ. In particular, we find that r increases with l (linearly with a crossover in the slope, as predicted), as well as with ϵ.

This result also leads to another interesting consequence. According to (16) $l_0 \to 0$ for $|\Lambda| \to \infty$ and $l_0 \to$ const for $|\Lambda| \to 0$, so that r diverges for both $|\Lambda| \to \infty$ and $|\Lambda| \to 0$. The optimal choice that minimizes r for a given level of noise σ corresponds to a finite value of Λ that can be found by trivial differentiation of (45).

In the conclusion of this section we should mention that (45) is expected to describe the minimal number of actuators for a broad class of scalar reaction-diffusion equations, not just the Swift-Hohenberg equation (1). The dependence on the choice of the evolution equation and specific parameters is contained entirely in the characteristic length l_0 and the coefficient C. The characteristic length can be computed using (12) and describes the linear part of the evolution equation, while the nonlinear part manifests through the coefficient C defined by (44). Computing C quantitatively for a general nonlinearity remains an open problem.

VI. FEEDBACK CONTROL OF PATTERNS

So far we have focused on controlling the uniform state. However, one might also be interested in using feedback to select one of the patterned (nonuniform) states, such as (3), that exist above the onset of primary instability. Without feedback the Swift-Hohenberg equation (1) typically evolves toward a periodic state ϕ_q with the base wave number q near the center of the unstable band, selected as a result of nonlinear competition involving secondary instabilities. In this section we restrict our attention to systems with periodic boundary conditions, for which the eigenmodes of the open loop system are given by (25). Therefore the infinite domain results summarized in Sec. II apply with the restriction that the base wave number has to be quantized.

A. Pattern selection

Localized feedback control can be used to bias the pattern selection in favor of a particular state with minor modifications. Indeed, a laterally confined system possesses a finite discrete set of unstable modes f_m, $a \leqslant |m| \leqslant b$ for any $\epsilon > 0$ (see Fig. 9). The feedback designed to stabilize the uniform state suppresses the growth of all these modes by shifting their wave numbers into the stable band. If the feedback for one of the originally unstable modes is turned off, e.g., we set $K^1_{\pm m}=0$, then the mode m will start to grow, until nonlinear saturation sets in, resulting in a stationary pattern (3) with the base wave number q_m. Since, for moderate ϵ, all higher harmonics $3m, 5m, \ldots$ of the mode m lie in the stable band, the feedback will change neither their temporal dynamics nor their saturated amplitudes.

Furthermore, we expect the feedback to be able to suppress one pattern (e.g., m "rolls") in favor of a different pattern (e.g., n rolls) by making $\lambda'_m < 0$ and setting $K^1_{\pm n}=0$, so that $\lambda'_{\pm n}=\lambda_{\pm n}$. This pattern switching is expected to work only for reasonably small ϵ, since the amplitude of the saturated state, and with it the deviation from the uniform state, relative to which the feedback is computed, scales like $\epsilon^{1/2}$. For larger values of ϵ the nonlinear terms in (1) become significant enough to invalidate the linear stability analysis and to lead control failure.

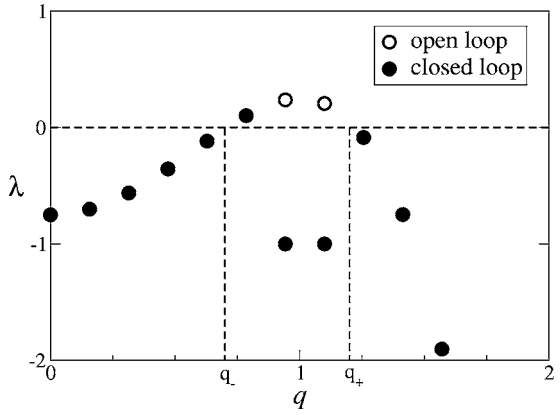

FIG. 9. The eigenvalue spectrum of the Swift-Hohenberg equation with $\epsilon=0.25$. The closed loop eigenvalues are chosen such that the five "roll" pattern is selected on the domain of size $l=40$.

The pattern selection and switching based on the approach described in this section are illustrated in Fig. 10. The initial condition is taken as the uniform state ϕ_0 with a small amount of broad spectrum noise added to it. Initially, the feedback is chosen to suppress all unstable eigenmodes except $f_{\pm 5}$, leading to the emergence of a five roll pattern. After that pattern has saturated, the feedback is switched to suppress all modes except $f_{\pm 7}$, resulting in the five roll pattern being replaced with a seven roll pattern.

As expected, the pattern selection becomes unreliable for large values of ϵ, producing stationary but mildly disordered patterns (not shown). Since the asymptotic state in this case differs from the target nonlinearly saturated pattern (3), the feedback signal does not vanish even for very large times. This is in contrast to all other instances considered in this paper, where the feedback disappears when the target state is reached.

B. Suppression of secondary instabilities

As is well known, the periodic patterns ϕ_q near the edges of the unstable wave number band are unstable towards the

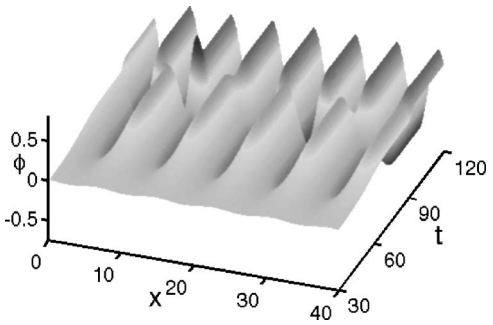

FIG. 10. Pattern switching from a five roll to a seven roll state for a system with four actuators, $l=40$ and $\epsilon=0.25$. The initial condition was chosen as a random noise with magnitude $\sigma=10^{-3}$.

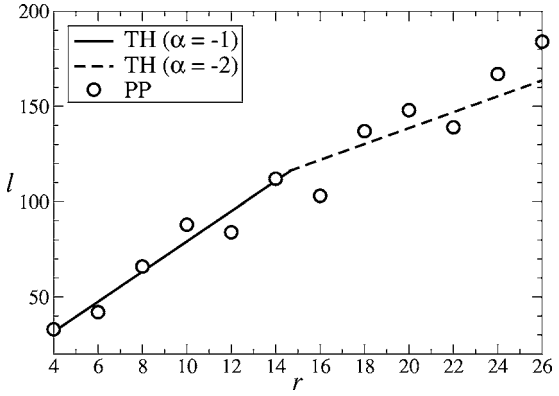

FIG. 11. Length l at which the control of a steady patterned state fails for a given number r of actuators. The wave number q lies in the unstable band, near q_+. The initial disturbance is of magnitude $\sigma=10^{-3}$ and $\epsilon=0.75$. New closed loop eigenvalues are chosen to lie in the interval $\lambda_k' \in [-2,-1]$. For comparison we also show the scaling result (45) for the uniform target state with a crossover from $\alpha=-1$ to $\alpha=-2$ and $\Lambda=-1.5$, chosen as the mean of the λ_k'.

Eckhaus instability (see Sec. II). This secondary instability can also be suppressed using localized feedback control (we will restrict our attention to the multiple actuator case here). The computation of the feedback gain again starts with rewriting the closed loop evolution equation (21) for disturbances $\hat{\phi}=\phi-\phi_q$ about the target pattern:

$$\partial_t\hat{\phi}=\epsilon\hat{\phi}-(1+\partial_x^2)^2\hat{\phi}-3\phi_q^2\hat{\phi}-3\phi_q\hat{\phi}^2-\hat{\phi}^3+\sum_{p=1}^{r}d_p(x)u_p(t). \tag{46}$$

Just like in the case of the uniform target state, we can project the linearized version of this equation onto the basis of Fourier modes (25). Since these are not the eigenmodes of the evolution operator of the open loop system anymore, the corresponding Jacobian matrix A will not be diagonal (see Appendix D). Another way to look at this is by noting that the linearization of (46) contains an extra term $-3\phi_q^2\hat{\phi}$ which represents nonlinear coupling between the disturbance (wave number k) and the target pattern (base wave number q), producing secondary disturbances with wave number $\pm 2q\pm k$ manifesting as the off-diagonal terms in the Jacobian. These secondary disturbances will affect the linear stability of the pattern since, for k close to q the mode with wave number $2q-k$ lies inside the unstable band.

Our analytical approach cannot be easily extended to this case, however the feedback gain coefficients that can be easily computed numerically using standard pole placement techniques. Computing the length of the system for which the control with r actuators breaks down we again find that it is consistent with a linear dependence with a crossover in the slope (see Fig. 11). What is perhaps more unexpected, we find the slopes to be approximated well by the expression (45) derived for the uniform state [we take the crossover to be between the values of $\alpha=-1$ and $\alpha=-2$ here, because (46) contains a quadratic, instead of a cubic, nonlinearity]. This suggests that our description of the mechanism for the control breakdown is applicable in a more general context and hence the scaling relation (45) likely describes the actuator spacing irrespective of the target state.

VII. CONCLUSIONS AND OUTLOOK

To summarize, we have shown that a broad class of spatially homogeneous extended systems—scalar one-dimensional reaction-diffusion PDEs-can, in principle, be controlled (or more precisely, their uniform and patterned states can be made linearly stable) by applying feedback at a few spatial locations with the only restriction that these locations have to satisfy the stabilizability condition. The tradeoff, compared with control schemes employing spatially continuous feedback (so-called fully actuated systems), is that the basin of attraction of the uniform state shrinks exponentially fast with increasing distance between actuators due to a strong transient growth of both initial and spontaneous disturbances. As a result, despite formal stability, systems controlled by a sparse array of actuators become extremely sensitive to noise, if the distance between actuators exceeds a certain characteristic distance specific to a particular system. This exponential sensitivity is independent of the type of the evolution equation or the choice of feedback and effectively sets a limit on the minimal number of actuators per unit length of the system in the presence of noise.

Noise sensitivity, and hence the minimal number of actuators is also independent—for systems of length $l \gg l_0$—on the choice of boundary conditions. Since there is no mean flux and the diffusion is the only effective transport mechanism, the influence of boundary conditions (any boundary conditions) can extend no further than the characteristic length l_0.

Noise sensitivity can be reduced, and hence the robustness of control improved, by either using a denser array of actuators or, to a lesser degree, by an appropriate choice of the eigenvalues of the closed loop system. The optimal choice of the new eigenvalues which leads to the smallest transient amplification depends on a delicate balance between the strength of the feedback gain and the time required to suppress a disturbance. The explicit analytical solutions for the feedback gain and the scaling relations for the transient amplification factor presented in this paper should help obtain a deeper insight into control theoretic methods, such as H_∞ control [28], whose objective is to increase robustness with respect to worst-case disturbances.

Furthermore, in computing a stabilizing feedback we used the knowledge of the system state on the whole domain $0<x<l$. This requirement can be easily relaxed by introducing a finite number of sensors that can measure the local state of the system at an array of points inside the domain. The feedback can then be computed using the state estimate constructed based on these spatially localized measurements. Mathematically, the control problems and the state estimation problems are dual, so by solving the former we also solve the latter [18]. As a result, one finds that the transient amplification should scale like

$$\gamma \sim e^{l/rl_0+l/pl_0}, \tag{47}$$

where r and p are the number of actuators and sensors, respectively, so that by using as many sensors as we have

actuators halves the characteristic length of the system.

Finally, while we restricted ourselves to evolution equations for scalar fields in one spatial dimension, we fully expect the main qualitative results presented here, such as the fast growth of the minimal number of actuators with the distance from the onset of primary instability, to be applicable also to vector or tensor fields and in higher dimensions (e.g., to the Boussinesque equations for Rayleigh-Bénard convection in a three-dimensional cell), thus providing an explanation to the empirical observations of Tang and Bau [4] that the control fails much sooner than the theoretical estimates [5] based on what the spatially continuous feedback would imply.

APPENDIX A: COMPUTING FEEDBACK FOR A SINGLE ACTUATOR

The matrix M in (8) is the Jacobian of the closed loop system and can be represented as the sum of the Jacobian $A=\mathrm{diag}(\lambda_1,\lambda_2,\lambda_3,\ldots)$ of the open loop system and the matrix

$$Q=\begin{pmatrix} K_1 & K_2 & K_3 & \cdots \\ -K_1 & -K_2 & -K_3 & \cdots \\ K_1 & K_2 & K_3 & \vdots \\ \vdots & \vdots & \vdots & \ddots \end{pmatrix} \tag{A1}$$

representing the action of the feedback. Our goal here is to find a set of coefficients K_m which will render the matrix M stable.

For a system of a given length l, we only have a finite number of positive eigenvalues corresponding to unstable modes of the open loop system. We will assume that $\lambda_n \geqslant 0$ for $n=a,\ldots,b$ and $\lambda_n<0$ otherwise (see Fig. 1). The eigenvalues λ_n can always be reindexed to achieve such an ordering. To render the matrix M stable, we only need to make these $s=b-a+1$ eigenvalues negative. (We assume for simplicity that the eigenvalues of both the closed loop and the open loop system are real; generalization to the case of complex eigenvalues is straightforward.) This can be achieved by setting all $K_m=0$ with the exception of $K_a,K_{a+1},\ldots,K_b$. To see this, let us write the matrix M in block form as

$$M=\begin{pmatrix} A_1 & Q_1 & 0 \\ 0 & A_s+Q_s & 0 \\ 0 & Q_2 & A_2 \end{pmatrix}. \tag{A2}$$

A_1 and A_2 denote the diagonal matrices containing the stable eigenvalues of A, A_s is the part of A containing the s unstable eigenvalues, and Q_1, Q_2, and Q_s are the respective nonzero blocks of (A1). The block structure of (A2) shows that the change in the eigenvalues of A_s through an appropriate choice of Q_s does not affect the rest of the eigenvalues of M. We, therefore, need to focus on the s-dimensional block matrix $M_s=A_s+Q_s$ and choose the coefficients $K_a,\ldots,K_b$ such that M_s becomes stable. This automatically renders the infinite matrix M stable.

The coefficients K_m can be computed analytically. To that end, consider choosing the s new negative eigenvalues of M_s as a sequence $\lambda'_a,\ldots,\lambda'_b$. We then need to find K_m that satisfy the set of equations

$$\det(M_s-\lambda'_m I)=0, \quad m=a,\ldots,b. \tag{A3}$$

Due to the special structure of (A1), one can solve (A3) for K_m and obtains the result (10).

APPENDIX B: COMPUTING FEEDBACK FOR A PAIR OF ACTUATORS

Projecting the linearization of the evolution equation (1) onto the basis (18) we obtain

$$\dot{\Phi}_n=\lambda_n\Phi_n-\sum_{m=1}^{\infty}[(-1)^m+(-1)^n]K_m\Phi_m\equiv(M\Phi)_n$$

where $\Phi_n(t)$ and K_n are again the Fourier coefficients of $\phi(x,t)$, and $k(x)$, respectively, defined as in (9). The matrix $M=A+Q$ is again composed of the Jacobian $A=\mathrm{diag}(\lambda_1,\lambda_2,\lambda_3,\ldots)$ and

$$Q=\begin{pmatrix} 2K_1 & 0 & 2K_3 & \cdots \\ 0 & -2K_2 & 0 & \cdots \\ 2K_1 & 0 & 2K_3 & \cdots \\ \vdots & \vdots & \vdots & \ddots \end{pmatrix}. \tag{B1}$$

Repeating the procedure described in Appendix A yields the result (19).

To obtain the scaling of the feedback gain with l, we again rewrite (19) in exponential form

$$|K_m|=\exp\left\{\ln\frac{|\lambda_m-\lambda'_m|}{2}+{\sum_p}'\ln\frac{|\lambda_m-\lambda'_p|}{|\lambda_m-\lambda_p|}\right\} \tag{B2}$$

and approximate the sums with integrals in the large l limit. Integrating over the unstable wave number band, we obtain to leading order in l

$$|K_m|\sim\exp\left\{\frac{l}{2\pi}\left(\int_{q_-}^{q_+}\ln\frac{|\lambda_m-\lambda'(q)|}{|\lambda_m-\lambda(q)|}dq\right)\right\}, \tag{B3}$$

from which (20) immediately follows upon substitution of $\lambda_m=\epsilon$.

APPENDIX C: COMPUTING FEEDBACK FOR MULTIPLE ACTUATORS

Our choice (24) of the individual feedback gains means that the respective Fourier coefficients K_m^p can be expressed in terms of the Fourier coefficients K_m^1

$$K_m^p=K^1_{-(-1)^p m}\exp\left\{-i\frac{\pi m}{r}[2p-1+(-1)^p]\right\}. \tag{C1}$$

A similar relation exists for the Fourier coefficients of the influence functions (22):

$$D_n^p=\exp\left\{-i\frac{\pi n}{r}[2p-1+(-1)^p(2\Delta-1)]\right\}. \tag{C2}$$

Using these two relations, the evolution equation (26) can be written in the form

$$\dot{\Phi}_n = \lambda_n \Phi_n + \sum_{p=1}^{r} \sum_{m=-\infty}^{\infty} F_{nm}^{p} K_{(-1)^p m} \Phi_m, \tag{C3}$$

where we defined

$$F_{nm}^{p} = e^{\pi i/r[(2p-1)(m-n)+(-1)^p(m-2n\Delta+n)]} \tag{C4}$$

and dropped the superscript on K_m^1 for notational convenience. We can again write (C3) in the matrix notation

$$\dot{\Phi} = M\Phi = (A+Q)\Phi, \tag{C5}$$

where $A=\mathrm{diag}(\ldots,\lambda_2,\lambda_1,\lambda_0,\lambda_1,\lambda_2,\ldots)$ and Q is a matrix with elements

$$Q_{nm} = \sum_{p=1}^{r} F_{nm}^{p} K_{(-1)^p m}. \tag{C6}$$

Further manipulating (C6), one obtains

$$\begin{aligned} Q_{nm} &= e^{2\pi i/r(n-n\Delta)} K_m \sum_{p}^{even} e^{2\pi i/rp(m-n)} \\ &\quad + e^{2\pi i/r(-m+n\Delta)} K_{-m} \sum_{p}^{odd} e^{2\pi i/rp(m-n)} \\ &= [e^{2\pi i/rn(1-\Delta)} K_m + e^{-2\pi i/rn(1-\Delta)} K_{-m}] R_{mn}, \end{aligned} \tag{C7}$$

where

$$R_{mn} = \begin{cases} r, & \dfrac{2(m-n)}{r} = \text{integer} \\ 0, & \text{otherwise}. \end{cases} \tag{C8}$$

As (C7) and (C8) show, for a given number $r/2$ of actuator pairs, Q consists of $r/2\times r/2$ blocks of diagonal matrices, a pattern that has already emerged in (B1) for the case of two actuators.

To find the gain coefficients K_m, we can again split the matrix M into blocks containing positive and negative eigenvalues of the diagonal matrix A. Note that A has positive eigenvalues in the columns $[-b,-a]\cup[a,b]$ and negative eigenvalues in columns $(-\infty,-b)\cup(-a,a)\cup(b,\infty)$. We could reorder the Fourier coefficients Φ_n in (C3) to obtain a matrix with the same structure as (A2). A more convenient way is to define the matrix M_s such that it not only contains the positive eigenvalues but also the negative eigenvalues in the columns $(-a,a)$. We then have $2b+1$ eigenvalues λ_m in columns $[-b,b]$ which can be modified with an appropriate choice of $K_{-b},\ldots,K_b$. Replacing the eigenvalues λ_m with new eigenvalues λ_M' for $m=-b,\ldots,b$ we obtain a set of $2b+1$ equations $\det(M_s-\lambda_m' I)=0$. Since the open loop system is real, $\lambda_m=\lambda_{-m}$. To ensure that the feedback is also real, we must choose $\lambda_m'=\lambda_{-m}'$. Solving for K_m one finds that, if we leave the negative eigenvalues in columns $(-a,a)$ unchanged, the only nonzero coefficients are given by (28), explicitly showing that the gain function $k_1(x)$ [and hence $k_p(x)$] is real.

To obtain the large l scaling we again rewrite (28) as an exponential and obtain

$$|K_m| = \exp\left\{ \ln\left| \frac{2C_m}{r}(\lambda_m - \lambda_m') \right| + \sum_p{}' \ln \frac{|\lambda_m - \lambda_p'|}{|\lambda_m - \lambda_p|} \right\}. \tag{C9}$$

As previously, we approximate the sums by integrals and integrate over the unstable wave number band. Ignoring the subleading $O(\ln l)$ terms we obtain

$$|K_m| \sim \exp\left\{ \frac{l}{\pi r} \left(\int_{q_-}^{q_+} \ln \frac{|\lambda_m - \lambda'(q)|}{|\lambda_m - \lambda(q)|} dq \right) \right\}, \tag{C10}$$

which leads to (30) upon substituting $\lambda_m=\epsilon$.

APPENDIX D: COMPUTING FEEDBACK FOR THE PATTERNED STATE

The calculation of the feedback gain for the patterned state is essentially identical to that for the uniform state. The only modification required by the presence of the additional term $-3\phi_q^2\hat{\phi}$ is in the evolution equation (46). Denoting the corresponding matrix elements as

$$S_{mn} = -\frac{3}{l}\int_0^l f_m^*(x)\phi_q^2(x) f_n(x) dx, \tag{D1}$$

the evolution equation for the Fourier amplitudes (C5) has to be replaced with

$$\dot{\Phi} = (A+S+Q)\Phi \equiv M\Phi, \tag{D2}$$

where once again $A=\mathrm{diag}(\ldots,\lambda_2,\lambda_1,\lambda_0,\lambda_1,\lambda_2,\ldots)$ and Q is given by (C6).

Substituting (3) with $q=q_k$ and (25) into (D1) we find

$$\begin{aligned} S_{mn} = -\frac{3}{4}\sum_{jp} a_j a_p [&\delta_{k(j+p),n-m} + \delta_{k(j-p),n-m} + \delta_{-k(j+p),n-m} \\ &+ \delta_{-k(j-p),n-m}] \end{aligned} \tag{D3}$$

and, since j, p, k, m, and n are all integers (with j and p odd and positive), the only nonzero elements of S are

$$S_{m,m+2nk} = -\frac{3}{4}\sum_p a_p (a_{2|n|-p} + a_{p+2|n|} + a_{p-2|n|}), \tag{D4}$$

with any integer n.

[1] M. Gad-El-Hak, *Flow Control: Passive, Active, and Reactive Flow Management* (Cambridge University Press, Cambridge, 2000).
[2] N. Garnier, R. O. Grigoriev, and M. F. Schatz, Phys. Rev. Lett. **91**, 054501 (2004).
[3] B. G. Levi, Phys. Today **54**(9), 18 (2001).
[4] J. Tang and H. H. Bau, J. Fluid Mech. **363**, 153 (1998).
[5] J. Tang and H. H. Bau, Proc. R. Soc. London, Ser. A **447**, 587 (1994).
[6] R. O. Grigoriev, Physica D **140**, 171 (2000).
[7] M. C. Cross and P. C. Hohenberg, Rev. Mod. Phys. **65**, 851 (1993).
[8] P. Christofides, *Nonlinear and Robust Control of PDE Systems: Methods and Applications to Transport-Reaction Processes* (Birkhäuser, Boston, 2001).
[9] L. N. Trefethen, A. E. Trefethen, S. C. Reddy, and T. A. Driscoll, Science **261**, 578 (1993).
[10] B. F. Farrell and P. J. Ioannou, J. Atmos. Sci. **53**, 2025 (1996).
[11] P. Schmid and D. Henningson, *Stability and Transition in Shear Flows* (Springer, New York, 2001).
[12] R. O. Grigoriev, M. C. Cross, and H. G. Schuster, Phys. Rev. Lett. **79**, 2795 (1997).
[13] D. A. Egolf and J. E. S. Socolar, Phys. Rev. E **57**, 5271 (1998).
[14] R. O. Grigoriev and A. Handel, Phys. Rev. E **66**, 067201 (2002).
[15] R. O. Grigoriev and A. Handel, Phys. Rev. E **66**, 065301(R) (2002).
[16] L. E. Howle, Phys. Fluids **9**, 1861 (1997).
[17] B. Bamieh, F. Paganini, and M. Dahleh, IEEE Trans. Autom. Control **47**, 1092 (2002).
[18] P. Dorato, C. T. Abdallah, and V. Cerone, *Linear Quadratic Control* (Krieger Publishing Company, Melbourne, 2000).
[19] K. Dutton, S. Thompson, and B. Barraclough, *The Art of Control Engineering* (Addison-Wesley, Boston, 1997).
[20] K. Morris, *Introduction to Feedback Control* (Harcourt Academic Press, San Diego, 2001).
[21] P. J. Schmid, Phys. Plasmas **7**, 1788 (2000).
[22] S. C. Reddy, P. J. Schmid, and D. S. Henningson, SIAM J. Appl. Math. **53**, 15 (1993).
[23] B. Bamieh and M. Dahleh, Phys. Fluids **13**, 3258 (2001).
[24] M. R. Jovanovic' and B. Bamieh, J. Fluid Mech. **534**, 145 (2005).
[25] E. Lauga and T. R. Bewley, J. Fluid Mech. **512**, 343 (2004).
[26] J. Baggett, T. Driscoll, and L. Trefethen, Phys. Fluids **7**, 833 (1995).
[27] J. Baggett and L. Trefethen, Phys. Fluids **9**, 1043 (1997).
[28] M. Green and D. J. N. Limebeer, *Linear Robust Control* (Prentice-Hall, New Jersey, 1995).